



# Employing a local framework and GIS to evaluate the flood risk index maps of Makassar City, Indonesia

Poppy Indrayani<sup>1</sup> · Ibrahim Djameluddin<sup>2,3</sup> · Yue Cai<sup>4</sup>

Received: 3 June 2022 / Accepted: 29 August 2023 / Published online: 21 September 2023  
© Saudi Society for Geosciences and Springer Nature Switzerland AG 2023

## Abstract

Flooding is a prevalent natural disaster in major cities throughout Indonesia. Over the past decade, Makassar City has experienced a severe increase in flood risk due to rapid and poorly controlled urbanization, as well as significant environmental degradation. The lack of reliable country-level flood hazard mapping at the sub-district level, coupled with limited local information and inadequate urban flood mitigation planning, further exacerbates the risk for residents. This paper aims to evaluate the vulnerability of social, physical, economic, and environmental aspects in the impacted areas of Makassar City to floods. The study employs a local methodological framework and geographic information system (GIS) to discern differences in flood risk levels across various areas. Leveraging available statistical and spatial data from the major flood that occurred in 2013, the research utilizes GIS spatial and temporal analysis to generate individual indicators and scores them using relevant parameters for vulnerability assessment in the local context. By combining the spatial parameters of the vulnerability index and flood hazard index, the study analyzes each component of the risk index and creates an overall risk index map. The distribution forms of specific risk levels and the percentage of risk areas for each sub-district are then examined. This analysis provides valuable insights to the local government, enabling better urban risk mitigation planning and accurate prioritization of necessary actions for each zone in Makassar City.

**Keywords** Makassar City · Risk index · Urban flood · Vulnerability · Spatial indicator

---

Responsible Editor: Biswajeet Pradhan

---

✉ Poppy Indrayani  
poppyindrayani@yahoo.com

Ibrahim Djameluddin  
ibedije@gmail.com

Yue Cai  
caihtm@yahoo.co.jp

- <sup>1</sup> Graduate School of Engineering, Fajar University, Prof. Abdurahman Basalamah No.101, Makassar City 90231, Indonesia
- <sup>2</sup> Faculty of Engineering, Hasanuddin University, Gowa Regency, Poros Malino KM 6, Bontomarannu 92171, Indonesia
- <sup>3</sup> Disaster Risk Reduction Research Center, Faculty of Engineering, Kyushu University, 744 Motooka Nishi-Ku, Fukuoka City 819-0395, Japan
- <sup>4</sup> School of Civil Engineering, Beijing Jiaotong University, No.3, Shangyuan Village, Haidian District, Beijing 100044, China

## Introduction

Flooding is the most common natural disaster in Indonesia (Parasati 2013; Riyanti et al. 2017). According to the National Disaster Management Agency (BNPB) in 2016, there were more than 1800 major natural disasters in the period 2005 to 2015, accounting for more than 78% of the total number of flood disasters. Floods have significantly impacted numerous communities, particularly in the urban areas of developing countries (Monirul et al. 2003; Rufat et al. 2015; White 2008). Makassar is one of Indonesia's major cities and a part of the Association of Southeast Asian Nations (ASEAN) Smart Cities Network (ASCN), aimed at improving the quality of life through infrastructure and promoting a healthy and sustainable environment. The local government of Makassar City is taking steps to prevent annual flood problems through an integrated approach to urban drainage spatial planning at the sub-district level.

**Fig. 1** Location map of Makassar City and boundaries of flood-impacted districts



However, the rapid and unprecedented growth of cities has also brought environmental challenges, including urban flood disaster management (Ehrlich and Holdren 1971; Kim and Gim 2020; Meydelin and Dyah 2020). Flood incidences in Makassar City are perennial occurrences and have been increasing in severity during the past decade due to its geographic location, rapid and poorly controlled urbanization, combined with severe environmental degradation (UN-Habitat 2014). According to data compiled by the Regional Disaster Management Agency (BPBD) in 2014, one of the major floods that occurred in January 2013 affected over 100,000 people overall and covered an area of around 3000 hectares. Urban flooding in developing countries is a common occurrence that seems to be worsening for several widely recognized reasons. Although several factors might lead to flooding, the first thing that typically triggers it is a high-intensity rainfall event, either directly over the city or in its catchment (Rana and Routray 2018). Increased urbanization, reduced water retention capacity, outdated urban drainage design, blocked drains, and land subsidence exacerbate the impact of increased river discharges and resultant flooding (Hoyer et al. 2011).

Additionally, flooding in coastal areas is frequently a two-directional occurrence with floods from the sea during high tide events and storm surges paired with upstream flooding from river flow (Sandhyavitri et al. 2019).

Numerous methodologies have been proposed for flood hazards and risk studies. Tehrany et al. (2014a) applied the combination of weights of evidence and a support vector machine model for flood vulnerability mapping. Moreover, Tehrany et al. (2014b) integrated bivariate and multivariate statistical models for flood susceptibility analysis. In another study, Tehrany et al. (2015a) employed the support vector machine and frequency ratio method for flood susceptibility analysis and verification. Tehrany et al. (2015b) used a GIS-based support vector machine model with different kernel types to assess flood susceptibility. Hu et al. (2017) utilized disaster risk theory and a risk assessment index system, along with the GIS-based AHP method, for flood risk assessment in Fangshan District, Beijing, China. Ngo et al. (2018) studied the hybrid swarm-optimized multilayer neural network to predict flash floods using sentinel-1 SAR (synthetic aperture radar) imagery and

**Table 1** Flooded districts and the percentage areas for each sub-district

District		Sub-district		
Name	Area (ha)	Name	Area (ha)	Area (%)
Manggala	2210.75	Bangkala	375.75	17
		Tamangapa	763.5	34
		Manggala	350.25	16
		Antang	531.25	24
		Batua	190	9
Tamalanrea	3889	Tamalanrea Indah	503.25	13
		Tamalanrea Jaya	375.5	10
		Tamalanrea	389.25	10
		Kapasa	669.25	17
		Parangloe	1080.25	28
		Bira	871.5	22
Rappocini	613	Gunung Sari	375.25	61
		Karunrung	131.5	21
		Kassi Kassi	106.25	18
Panakkukang	927.5	Pampang	334.25	36
		Panaikang	304.25	33
		Paropo	127	14
		Tello Baru	162	17
Tallo	500.5	Buloa	95.25	19
		Tallo	62.75	13
		Lakkang	342.5	68
Biringkanaya	2021.25	Paccerrakkang	750	37
		Sudiang Raya	647.5	32
		Sudiang	623.75	31

geospatial data. Ghosh and Kar (2018) employed the Analytic Hierarchy Process (AHP) model to map flood hazards in the Malda district of West Bengal, India. Darabi et al. (2019) compared machine learning techniques, such as the Genetic Algorithm Rule-Set Production (GARP) and Quick Unbiased Efficient Statistical Tree (QUEST) models, to map the risk of urban flooding. Dano et al. (2019) used GIS-based analytical network for flood susceptibility mapping in Perlis, Malaysia. Khosravi et al. (2019) compared multi-criteria decision-making analysis and machine learning methods for flood susceptibility modeling. Chen et al. (2020) studied flood susceptibility modeling using a data-driven approach with the naive Bayes tree, alternating decision tree, and random forest methods. In the eastern Hindu Kush, Pakistan, Ullah and Zhang (2020) used frequency ratios to determine flood susceptibility areas. Roy et al. (2021) assessed the flood risk of the sub-Himalayan Jalpaiguri

region using a multi-criteria decision approach to prepare the flood susceptibility, vulnerability, and flood risk maps for the study area. With the advancement of computer science, artificial intelligence (AI) is being incorporated into many fields and applied for flood risk mitigation (Kasuni et al. 2021; Wang 2021; Zalnezhad et al. 2022). Additionally, Bose and Mazumdar (2023) applied the Integrated Valuation of Ecosystem Services and Tradeoffs-Urban Flood Risk Mitigation (InVEST-UFRM) model to understand the flood-like situation and find possible mitigation measures in the city of Kolkata. Iqbal et al. (2023) generated a high-resolution digital terrain model (DTM) based on unmanned aerial vehicle (UAV) photogrammetry and used a two-dimensional (2D) hydrodynamic model (HEC-RAS) to simulate flood processes in a floodplain environment of the Jamuna River in northern Bangladesh. Sahraei et al. (2023) developed a novel hybrid GIS-based multi-criteria decision-making approach for flood susceptibility analysis. However, it is worth noting that most of these studies primarily focus on statistical approaches for flood risk prediction, while paying less attention to overcoming the challenges posed by data limitations, illustrating real-world cases, and accurately defining flood risk zonation based on actual flood events.

In most cases, risk has been defined in relevance to the needs of various sciences that require disaster management methods (Adger and Kelly 1999; UNDP 2004). Many vulnerability frameworks aim to analyze vulnerability factors using mathematical statistics of historical disasters, coupling models, and method-based spatial analysis (Rehman et al. 2019; Chang et al. 2021). In general, flood risk assessment relies on mathematical models to establish the likelihood of a given event occurring with a certain degree of intensity in a specific location (Cutter and Finch 2008; Ahmad and Simonovic 2013). The use of geographic information system (GIS) can offer an advantage by synthesizing data and providing essential mapping of spatial relationships between hazards and vulnerabilities and the components at risk (Longley et al. 2001). The flood risk assessment map provides a general perspective of the region, indicating the likelihood of a flood tragedy occurring in particular locations (Dintwa et al. 2019). The central government of Indonesia provides a flood risk assessment map at the city level using three categories of risk (BNPB 2016). However, the study scale is small, and the areas plotted under each category are far too vague and broad to be useful in determining the flood risk in specific locations within a city (Siagian et al. 2014). Furthermore, the

**Fig. 2** Flood hazard index map generated from flood measurements in 2013

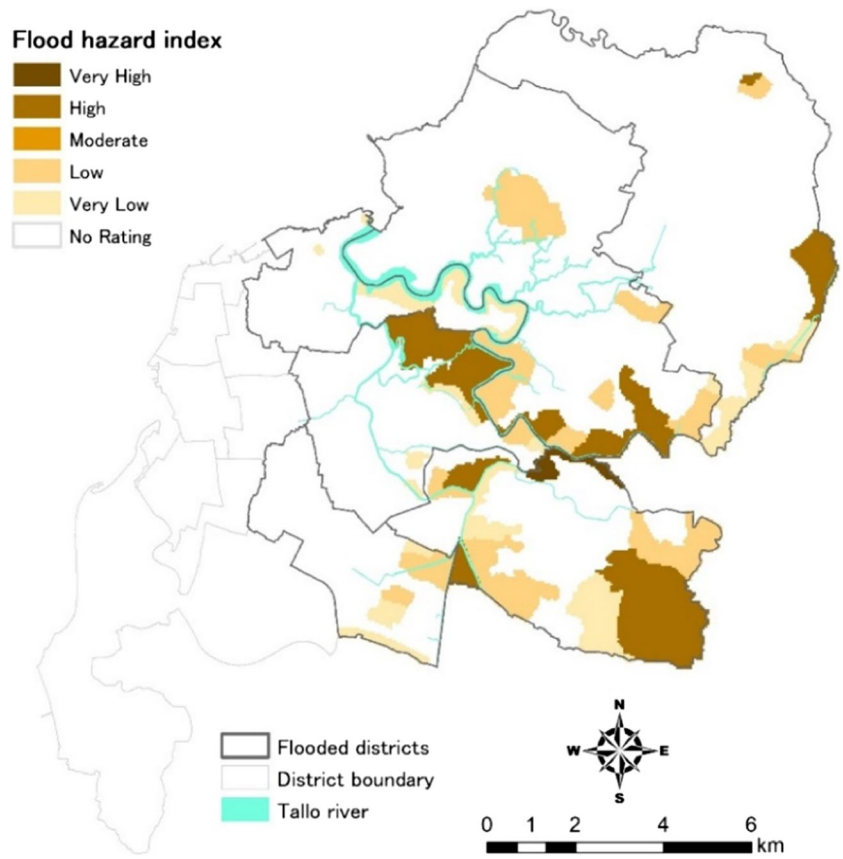


**Fig. 3** Research methodology flowchart

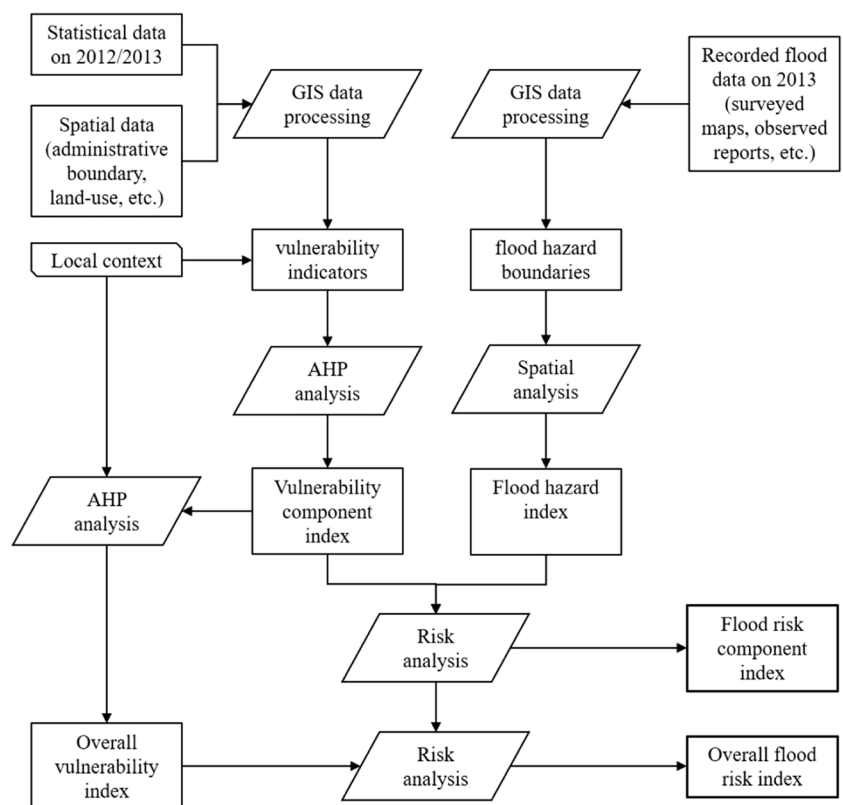
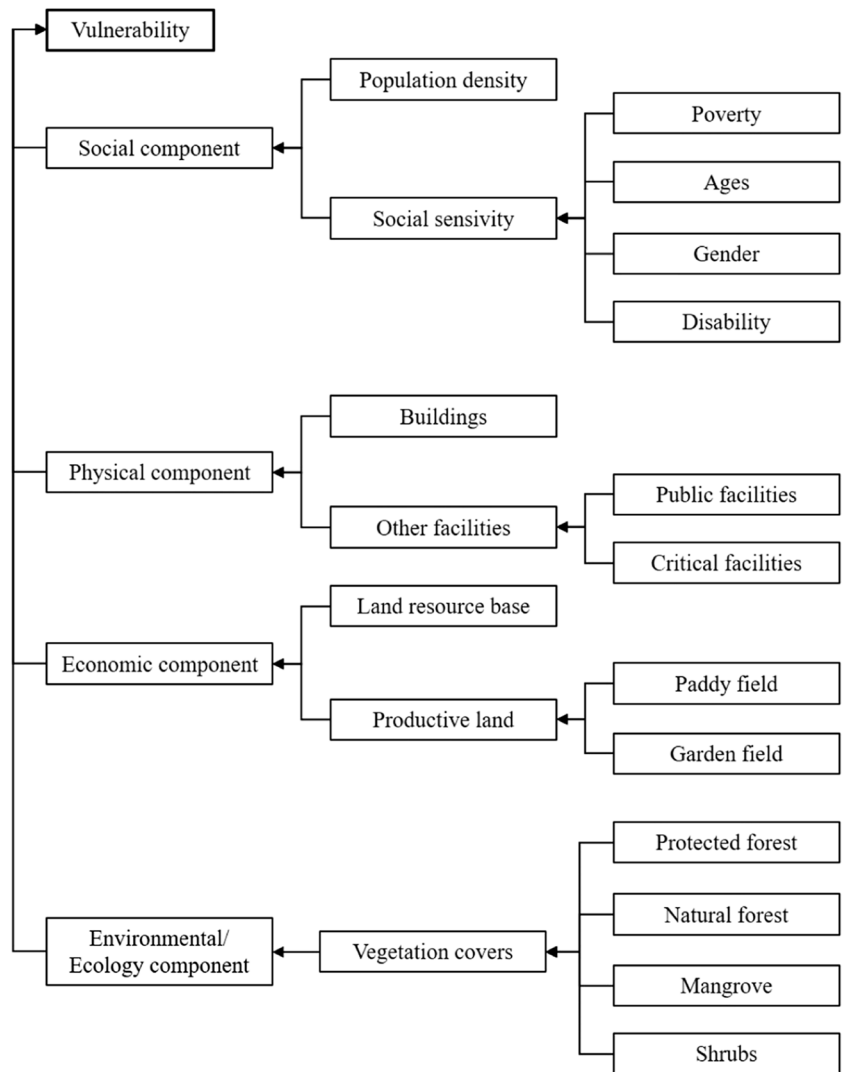


**Fig. 4** Conceptual framework for estimating vulnerability in the local context as a critical component of flood risk



lack of district and sub-district level information, along with the need for effective land use planning, flood early warning systems, and budget constraints, presents significant obstacles to flood hazard mitigation in developing countries.

In this study, we evaluate the vulnerability of social, physical, economic, and environmental aspects in the impacted areas in Makassar City to floods in 2013. Our aim is to discern the extent of flood risk level differences across the sub-districts. To address the challenges mentioned earlier, we propose a methodology to map flood hazard zones at the district and sub-district levels. The analysis includes assessing the distribution of specific risk levels and their percentage risk regions within each sub-district. The specific indicators are generated using GIS spatial and temporal analysis based on the available statistical data and geographical data from the same

time period, in accordance with the local methodological framework and methodology relevant to vulnerability assessment in Indonesia. Additionally, to establish proper baseline measurements for spatial planning strategies at

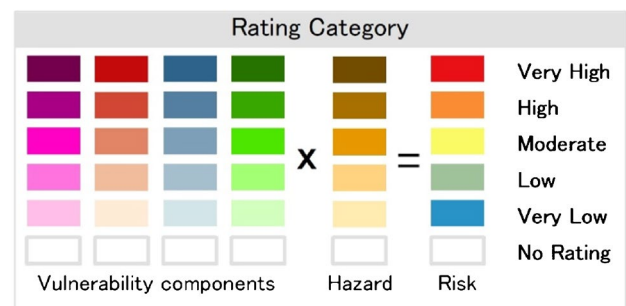


**Fig. 5** Risk index qualitative rating legend and illustration of risk levels

**Fig. 6** Classification definition of potential impacts according to the BNPB

Potential impacts			
Very low	Low to Moderate	Moderate to High	Very High
<i>Minimal disruption</i>	<i>Minor disruption</i>	<i>Significant disruption</i>	<i>Severe disruption</i>
Generally, no widespread impact, however, there may still be; •Isolated and minor flooding of low-lying land and roads. •Little or no disruption to travel although wet road surfaces could lead to difficult driving conditions.	•Localized flooding of land and roads. •Localized flooding could affect individual properties. •Localized disruption to key sites identified in flood plans (e.g. public utilities). •Local disruption to travel, longer journey times.	•Flooding affecting properties and parts of communities. •Damage to buildings is possible. •Potential disruption to infrastructure (e.g. utilities). •Disruption to the travel network is expected. A number of roads are likely to be closed.	•Widespread flooding affects a significant number of properties and communities. •Danger to life from fast-flowing and/or deep water. •Widespread disruption or loss of infrastructure (e.g. utilities). •Large scale evacuation may be required. •Severe disruption to travel networks.

the sub-district level, the GIS analysis based on the grid-mesh system determines the components and composite risk index levels, along with the location and percentage of risk regions. This approach will enable the local government to plan for disaster mitigation more precisely, focusing resources on areas with actual risk, leading to lower mitigation and early warning system costs.

## Material and methods

### Study area

#### Characteristics of flood threat

Makassar City is located on the southwestern coast of the island of South Sulawesi. Based on the statistical demographic data provided by the municipality in

2012, the population reached approximately 1.4 million people, with an average population growth rate of about 1.5% over the last 10 years. The city’s topography includes flat areas with a slope of 0–2° and undulating land with a slope of 3–15°, comprising lowlands at an altitude ranging from 0 to 40 m above sea level. Due to topography conditions, many areas regularly experience flooding during the rainy season, especially when heavy rainfall coincides with rising tide. The Tallo rivers primarily run through the city, covering around 81% of the watershed area. The watershed area of the river is about 407 km<sup>2</sup>, originating at a ground elevation of approximately 725 m, and the length of the main river is approximately 72 km. Tallo river flows through the coastal area of Makassar City, passing through the districts of Manggala, Panakukang, Rappocini, Tallo, Tamalanrea, and Biringkanaya (Fig. 1). The riverbank in its natural state without flood control measures. The widespread

**Fig. 7** Individual indicator values for each component of vulnerability

Component	Vulnerability					
	Exposure		Susceptibility		Resilience	
	Indicator	Definition	Indicator	Definition	Indicator	Definition
Social	Population density (inhabits/km <sup>2</sup> )	People per km <sup>2</sup>	% of age (<5 and >65 years)	Percentage of children under 5 or elderly above 65	% of disabled peoples	Percentage of any kind of disabilities
	% of poverty	Percentage of the population under poverty	% of gender (women)	Percentage of women		
Physical			Building codes	Building values are divided into houses, public facilities, and critical facilities (e.g. water supply)		
	Productive land	Income-producing unit (e.g. farm)				
Economic	Land resource base (PDRB)	Total available local budget				
Environmental	Vegetation covers	Protected forest, natural forest (e.g. mangrove in ha)				

**Table 2** Index conversion parameters for social vulnerability indicators

Parameter	Code	Weight (%)	Value			Score
			Low	Medium	High	
Population density (inhabits/km <sup>2</sup> )	E1	60	< 500	500–1000	> 1000	$X_j$
Percentage of poverty (%)	E2	10	< 20	20–40	> 40	
Percentage of ages (%)	S1	10				
Percentage of gender (%)	S2	10				
Percentage of disability (%)	R1	10				

**Table 3** Index conversion parameters for physical vulnerability indicators

Parameter	Code	Weight (%)	Value			Score
			Low	Medium	High	
Houses (in million rupiah)	S3a	40	< 400	400–800	> 800	$X_j$
Public facilities (in million rupiah)	S3b	30	< 500	500–1000	> 1000	
Critical facilities (in million rupiah)	S3c	30	< 500	500–1000	> 1000	

residential developments in the Tallo watershed have contributed to significant rainfall-induced surface water flow and the problem of groundwater intrusion. As a result, floods caused by increased surface water flow are spreading to more sub-districts. Historical records show that from 1979 to 2013 the city witnessed the maximum rainfall with an average value of 156.4 mm per day. Generally, floods occur from December to February, which is the period of the highest rainfall every year. The overflow of the Tallo river, the inability of the water catchment area to absorb the volume of surface water, and the lack of areas with a drainage system are major factors contributing to flooding.

**Flood hazard index map**

Makassar City, predominantly comprising the districts of Biringkanaya, Tamalanrea, Tallo, Manggala, Rappocini, and Panakukkang, experienced floods in January 2013. Table 1 shows the names of the flood-impacted districts and the estimated percentage areas of the sub-districts. The first flood hazard map for Makassar City was created in 2013 through a coordinated survey conducted by the municipality and the BPBD. The map utilized data from site measurements taken in 2013 and records of previous flooding incidents in the city. It was constructed based on two primary factors: the likelihood

**Table 4** Index conversion parameters for economic vulnerability indicators

Parameter	Code	Weight (%)	Value			Score
			Low	Medium	High	
Productive land (e.q., paddy field, garden field) (in million rupiah)	E3	60	< 50	50–200	> 200	$X_j$
Land resource base (PDRB) (in million rupiah)	E4	40	< 100	100–300	> 300	

**Table 5** Index conversion parameters for environmental vulnerability indicators

Parameter	Code	Weight (%)	Value			Score
			Low	Medium	High	
Protected forest (ha)	E5a	40	< 20	20–50	> 50	$X_j$
Natural forest (ha)	E5b	40	< 25	25–75	> 75	
Mangrove (ha)	E5c	10	< 10	10–30	> 30	
Shrubs (ha)	E5d	10	< 10	10–30	> 30	

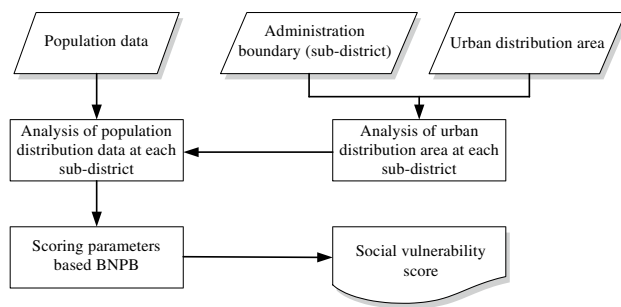


**Fig. 8** Flowchart of GIS analysis for calculating the social vulnerability score

of a threat (border flooded areas) and the severity of impacts (flood depths) documented from previous yearly flood catastrophes (UNISDR 2017). This flood hazard map aimed to provide highly accurate city-scale flood hazard maps in Eastern Indonesia. In this study, the established flood hazard map is translated into five danger classes (very low, low, moderate, high, and very high) based on the local context (Fig. 2). This translation allows for the creation of a flood hazard index map that is comparable in dimensions and suitable for use in spatial risk analysis.

## Risk analysis

### Flood risk calculation

Flood hazard risk, in the most general terms, is often defined as the likelihood (or probability) of a flood hazard event happening multiplied by the expected consequence if a flood hazard event occurs. In the flood risk index, risk is defined as the potential for negative impacts resulting from a flood hazard (Chen et al. 2013). The risk equation comprises two components: a flood hazard component and a vulnerability component. Vulnerability serves as the consequence-enhancing factor, measured by the anticipated loss of property value, population, and/or agricultural value. Demographic factors are examined to assess the social community's susceptibility to flood hazards, as well as its ability to prepare for, adapt to, and recover from their effects (Cutter 1996; Cutter et al. 2003). Preparation of the risk calculation index requires the local context framework and spatial analysis (Flanagan et al. 2011; Muller et al. 2011; Bigi et al. 2021). In this case study, the calculation model of flood risk considers the local methodological framework and approach provided by the BNPB (Fig. 3). This

approach acknowledges that vulnerability has specific spatial, socio-economic-demographic, environmental, and physical contexts, which pose challenges to modeling vulnerability as part of risk evaluation and risk management in the context of disaster risk management in Indonesia (Fig. 4). It fulfills the need for standards in estimating vulnerability as a critical component of risk evaluation in Makassar City.

### Scores and ratings

In the risk calculation, each component is represented by a unitless index score at the same level (Schmidtlein et al. 2008). These scores, one for hazard and another for vulnerability, are combined to calculate the overall flood risk index score, measuring the flood risk to all vulnerability components. Additionally, the risk index score is provided as both an overall score from the summation of all vulnerability components and as scores where each vulnerability component is considered separately. The calculations are conducted separately at the sub-district level, making the scores relative only within their level. All individual indicator scores are constrained to a range from the lowest to the highest possible value (Spielman et al. 2020). To achieve this range, the values of each component undergo rescaling using min–max normalization, preserving their spatial distribution while simplifying analysis. For every score, a qualitative rating is assigned, describing the nature of the vulnerability component score compared to all other components at the same level. This qualitative assessment ranges from “Very Low” to “Very High” and provides valuable insights into the vulnerability component's relative position among the others. Because all ratings are relative, there are no specific numeric values that determine the rating. For instance, a physical vulnerability score could be 0.5 with a rating of “relatively low,” while its social vulnerability score may be 0.7 with a rating of “very low.” The ratings are intended to classify values for specific vulnerability components in relation to all other components at the same level. The finalized cluster of the lowest scores is assigned the rating “very low,” the next lowest cluster receives a rating of “relatively low,” and so on. In the application's maps and data visualizations, color schemes have been applied to represent the qualitative ratings. The risk index ratings use a diverging blue (very low) to red (very high) color scheme. Ratings for social vulnerability, physical vulnerability, economic vulnerability, and environmental vulnerability use sequential color schemes. In general, darker shading in



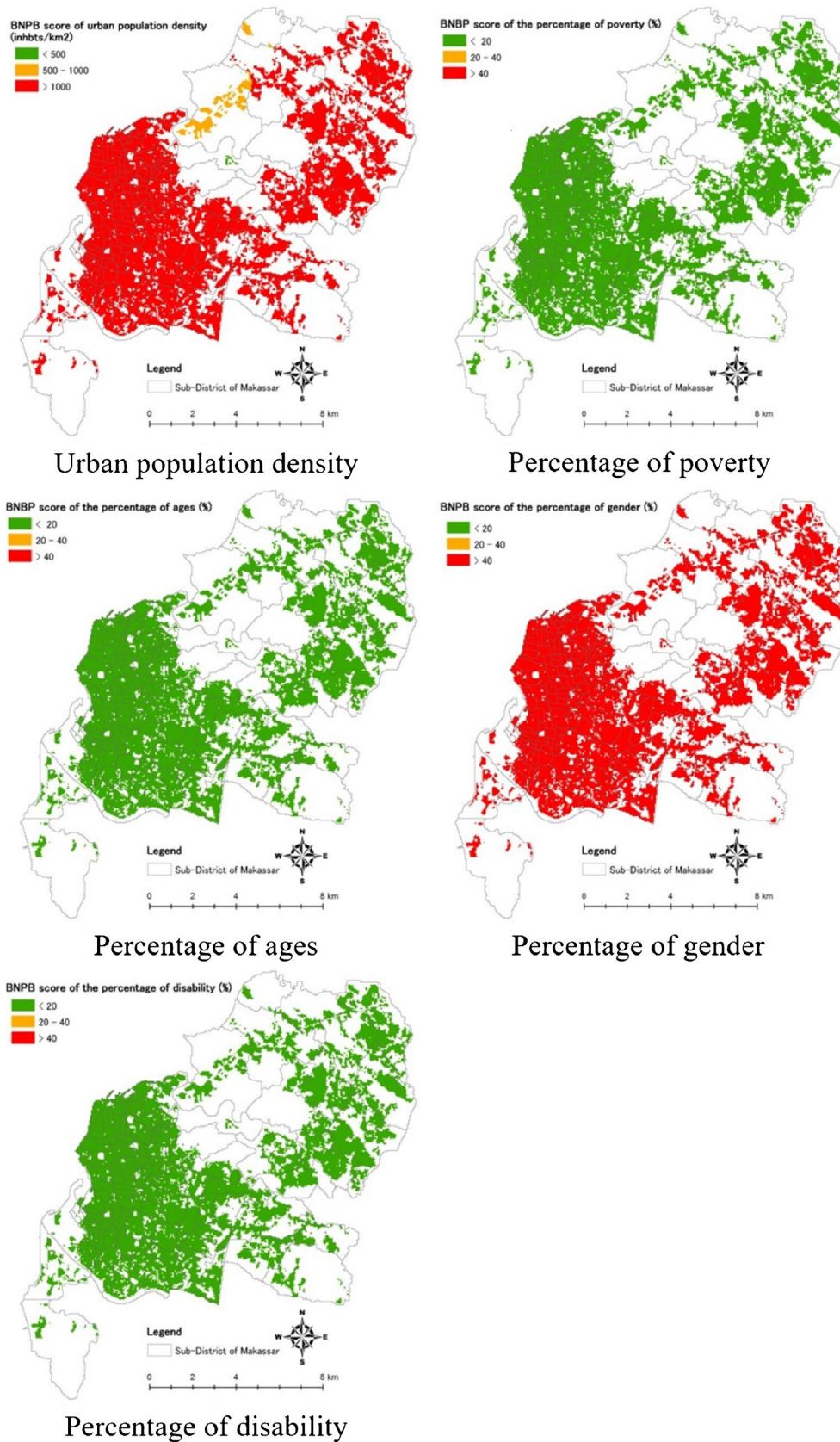
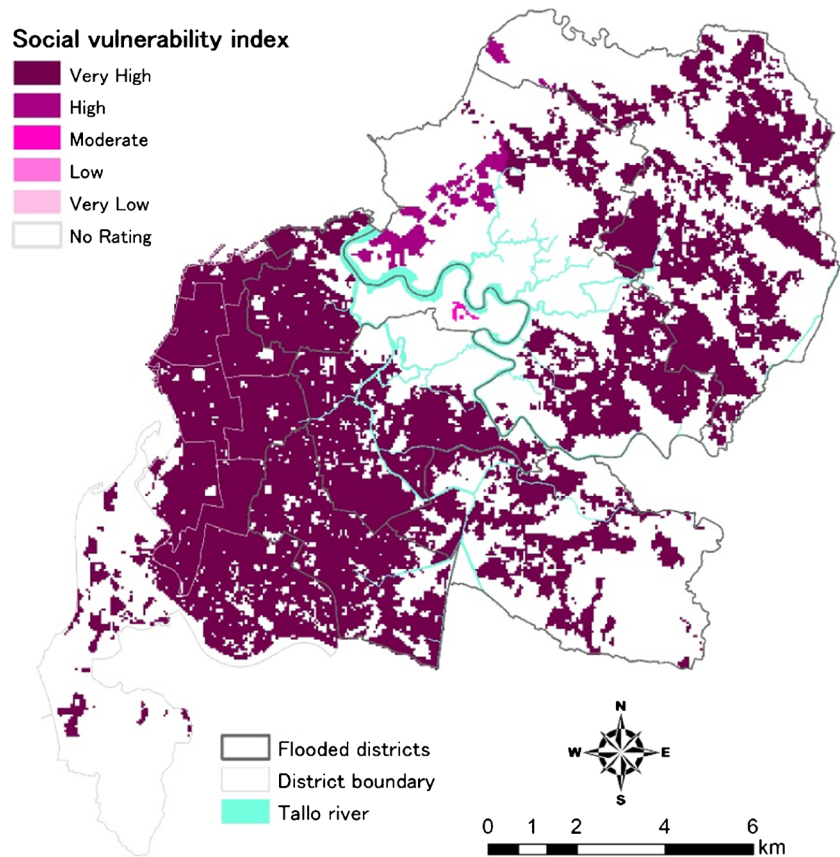


Fig. 9 Scoring of individual indicator maps for the social vulnerability component

**Fig. 10** Social vulnerability score



the map layers represents a higher contribution to overall risk. When source data are not available, or a score cannot be calculated, additional ratings are used and shown in white. The color schemes are shown in Fig. 5 with illustrative examples and rating categories. Scores of 0 (zero) or null values in the flood risk factors receive no ratings to reflect the logic behind the risk score. An area where the risk is zero either has no building value, population, or agriculture value exposed to the flood hazard. These areas are displayed in the application as having no expected risk. Furthermore, Fig. 6 shows the classification definition of potential impacts for the local context.

## Vulnerability analysis

### Individual indicators

The risk index assessment is based on four components: social vulnerability, physical vulnerability, economic vulnerability, and environmental vulnerability. Each vulnerability component contributes to either the likelihood or consequence aspect of risk (Hufschmidt 2011; Tate et al. 2021). The individual indicators for each

vulnerability component are summarized in Fig. 7. This local framework guides systematic assessments of vulnerability by considering key factors and various spatial dimensions: (1) Exposure (*E*) is calculated by considering the density of the population per sub-district area (*E1*), the percentage of the population under poverty (*E2*), the land resource base (*E3*), the extent of productive land (*E4*), and the percentage of the vegetation cover (e.g., protected forest, natural forest) (*E5*); (2) susceptibility (*S*) is calculated by considering the percentage of the number of children under five years old or elderly above 65 years (*S1*), the percentage of women per sub-district area (*S2*), and the number of buildings related to their structural value and importance (*S3*); and (3) resilience (*R*) is calculated by considering the number of disabled individuals (e.g., homeless, literacy rate, and handicap) for lack of resilience (*R1*).

### Social vulnerability

The social vulnerability score represents the relative level of social vulnerability for a given sub-district compared to all other sub-districts at the same level.

**Table 6** Risk assessment index for the social component at the sub-district level

Sub-district	Area (ha)	Flood risk		Percentage area at risk levels (%)				
		Area (ha)	%	VL	L	M	H	VH
Bangkala	375.75	231	61	79		21		
Tamangapa	763.5	605.75	79	90	8	2		
Manggala	350.25	169.75	48	79		21		
Antang	531.25	158	30	65	26			9
Batua	190	92.5	49	76		16	8	
Tamalanrea Indah	503.25	142	28	90		10		
Tamalanrea Jaya	375.5	273.25	73	79		13	8	
Tamalanrea	389.25	100.75	26	62	13	17	8	
Kapasa	669.25	51.25	8	47		53		
Parangloe	1080.25	7.5	1	27		73		
Bira	871.5	180	21	91		9		
Gunung Sari	375.25	81.25	22	40	47	3		
Karunrung	131.5	68	52	42	40	18		
Kassi Kassi	106.25	56.75	53	51	11	38		
Pampang	334.25	167	50	100				
Panaikang	304.25	160.25	53	80	16		4	
Paropo	127	27	21	14	86			
Tello Baru	162	48.25	30	67	14	9	10	
Buloa	95.25	4.5	5	38	62			
Tallo	62.75	6.25	10	32	68			
Lakkang	342.5	200.75	59	100				
Paccerakkang	750	196	26	75	21	4		
Sudiang Raya	647.5	118.25	18	75			25	
Sudiang	623.75	33.25	5	45		43	12	

A higher social vulnerability score indicates a higher risk. The indicators used for social vulnerability include population density, percentage of poverty, percentage of age, percentage of gender, and percentage of disability.

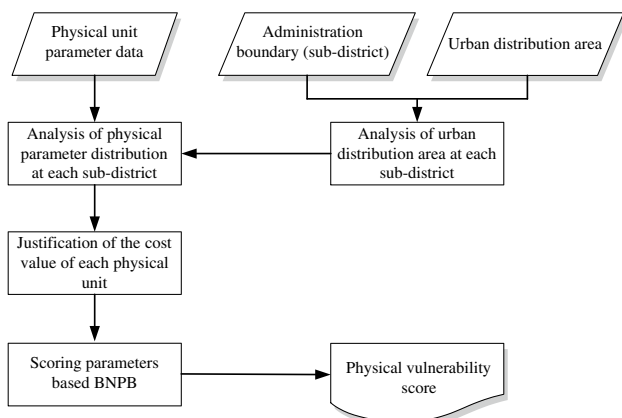


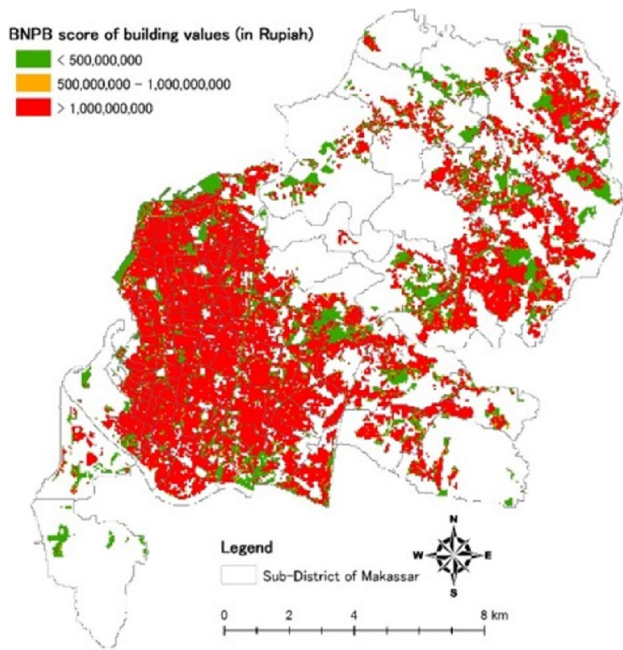
**Fig. 11** Flowchart of GIS analysis for calculating the physical vulnerability score

The index of social vulnerability is derived from the average weight of population density (60%), and the weight of social sensitivity (40%), which consists of percentages of poverty (10%), age (10%), gender (10%), and disability (10%). Index conversion parameters are described in Table 2. For practical implementation, the score is normalized by dividing the vulnerability value  $x_j$  by the number of vulnerability items, i.e., the maximum vulnerability value is 1. The normalized vulnerability is then calculated based on the equation:

$$X_j = \frac{x_j - \text{Min}(x_j)}{\text{Max}(x_j) - \text{Min}(x_j)} \tag{1}$$

where,

$X_j$  is the normalized value (ranging from 0 to 1) of the indicator  $j$  of a vulnerability factor ( $E, S, R$ );  $x_j$  is the value of the indicator  $j$ ;  $\text{Max}(x_j)$  and  $\text{Min}(x_j)$  represent the maximum and minimum values, respectively, of the indicators  $j$  for the vulnerability factor.



### Building classification costs

Fig. 12 Scoring of individual indicator maps for the physical vulnerability component

Thus, the normalized indicators were aggregated using the following equation, according to their respective factors:

$$VI_{\text{social}} = \sum_{j=1}^k W_j X_j \tag{2}$$

where  $VI_{\text{social}}$  is the composite indicator ( $E1, E2, S2, S3, R1$ );  $W_j$  is the weight of the indicator  $j$ ; and  $X_j$  is the normalized value of the indicator  $j$ .

### Physical vulnerability

The indicators used for physical vulnerability are building house density, availability of public facilities, and availability of critical facilities. House density is obtained by dividing the built area by the area of the sub-district (in hectares) and multiplying it by the unit price of each building code parameter. The index of physical vulnerability is derived from the average weight of house density (40%), availability of public facilities (30%), and availability of critical facilities (30%). Index conversion parameters are described in Table 3. The normalized indicators were aggregated using the following equation, according to their respective factors:

Fig. 13 Physical vulnerability score

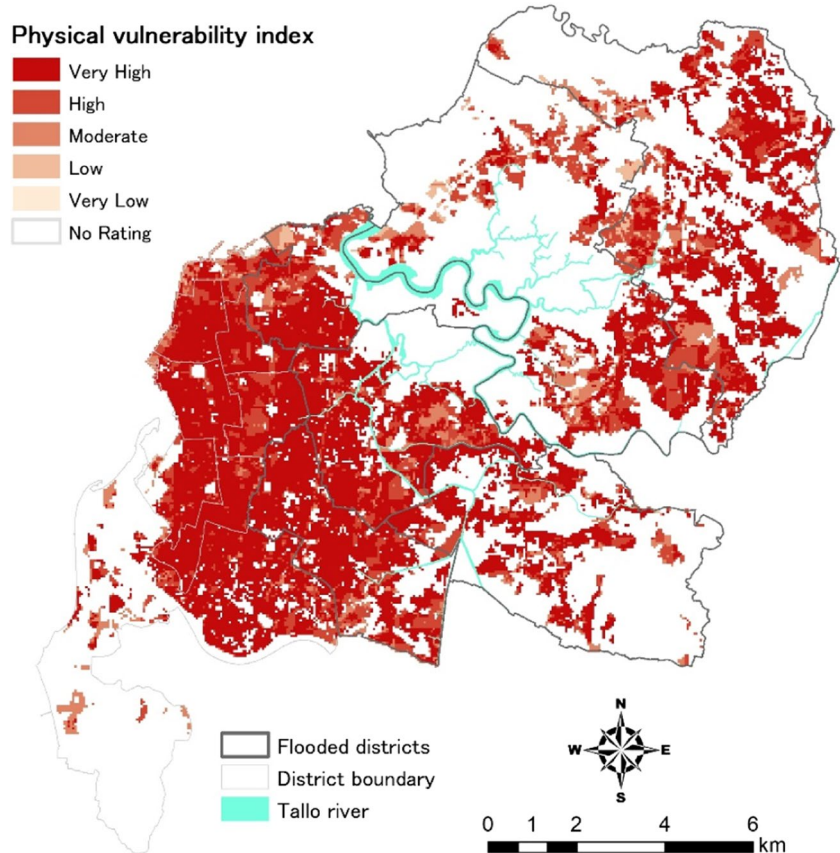


**Table 7** Risk assessment index for the physical component at the sub-district level

Sub-district	Area (ha)	Flood risk		Percentage area at risk levels (%)				
		Area (ha)	%	VL	L	M	H	VH
Bangkala	375.75	231	61	79	2	15	4	
Tamangapa	763.5	605.75	79	90	4	4		
Manggala	350.25	169.75	48	79	5	16		
Antang	531.25	158	30	65	15	12	1	7
Batua	190	92.5	49	76		9	12	3
Tamalanrea Indah	503.25	142	28	90		2	8	
Tamalanrea Jaya	375.5	273.25	73	79	2	13	5	1
Tamalanrea	389.25	100.75	26	62	11	10	17	
Kapasa	669.25	51.25	8	47		30	23	
Parangloe	1080.25	7.5	1	27		73		
Bira	871.5	180	21	91	1	8		
Gunung Sari	375.25	81.25	22	40	47	13		
Karunrung	131.5	68	52	42	40	18		
Kassi Kassi	106.25	56.75	53	51	13	36		
Pampang	334.25	167	50	100				
Panaikang	304.25	160.25	53	80	11	6	1	2
Paropo	127	27	21	14	71	15		
Tello Baru	162	48.25	30	67	8	12	3	10
Buloa	95.25	4.5	5	38	62			
Tallo	62.75	6.25	10	32	68			
Lakkang	342.5	200.75	59	100				
Paccerakkang	750	196	26	75	13	10	2	
Sudiang Raya	647.5	118.25	18	75		19	1	5
Sudiang	623.75	33.25	5	45		21	23	11

$$VI_{\text{physical}} = \sum_{j=1}^k W_j X_j \tag{3}$$

where  $VI_{\text{physical}}$  is the composite indicator ( $S3a, S3b, S3c$ ).

**Economic vulnerability**

The indicators used for economic vulnerability are the area of productive land (e.g., paddy fields, garden fields) measured in rupiah value and the land resource base of PDRB (gross regional domestic product) for the agriculture sector. The area of productive land can be obtained from the analysis of land use maps, and the PDRB of statistical data at the district and sub-district levels are analyzed. The index of economic vulnerability is derived from the weight of the area of productive land (60%), and the weight of the land resource base (40%). Index conversion parameters are described in Table 4. The normalized indicators were aggregated using the following equation, according to their respective factors:

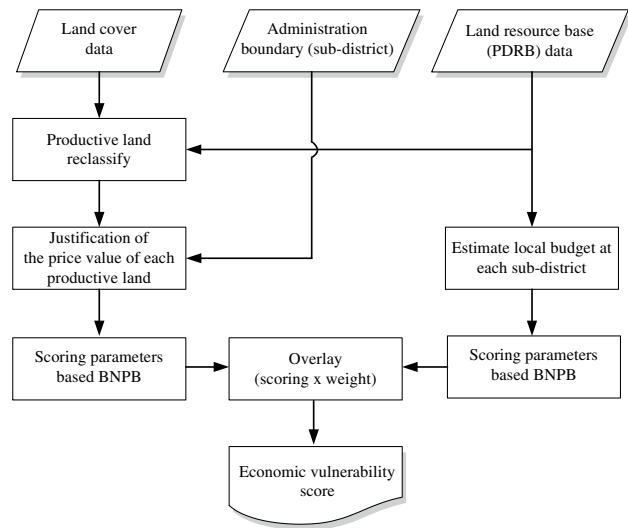


**Fig. 14** Flowchart of GIS analysis for calculating the economic vulnerability score

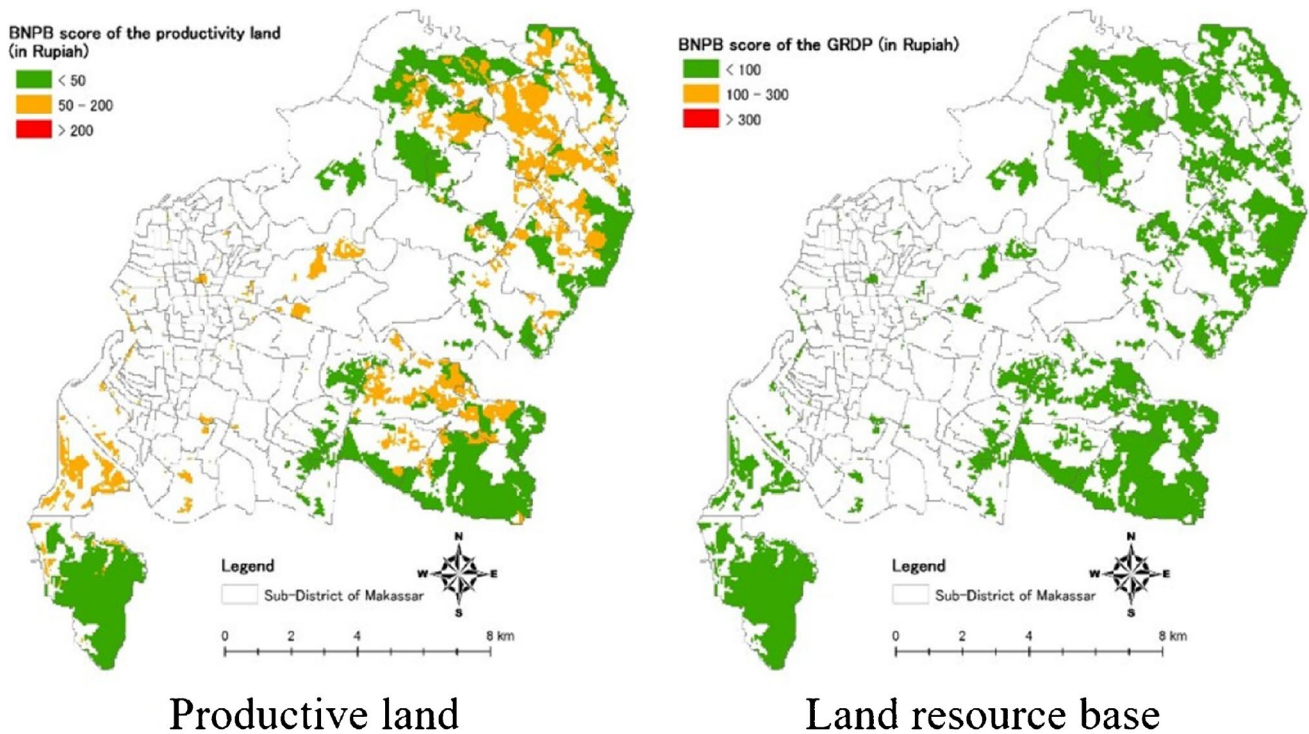


Fig. 15 Scoring of individual indicator maps for the economic vulnerability component

$$VI_{\text{economic}} = \sum_{j=1}^k W_j X_j \tag{4}$$

where  $VI_{\text{economic}}$  is the composite indicator ( $E3, E4$ ).

**Environmental vulnerability**

The indicators used for environmental vulnerability are protected forests, natural forests, mangroves, and shrubs. The index of environmental vulnerability is derived from the weight of the area of protected forest (40%), the weight of the natural forest (40%), the weight of the mangrove (10%), and the weight of shrubs (10%). Index conversion parameters are described in Table 5. The normalized indicators were aggregated using the following equation, according to their respective factors:

$$VI_{\text{environmental}} = \sum_{j=1}^k W_j X_j \tag{5}$$

where  $VI_{\text{environmental}}$  is the composite indicator ( $E5a, E5b, E5c, E5d$ ).

**Overall vulnerability**

In this study, it effectively communicates that spatial–temporal information related to the four components

of flood vulnerability is presented and processed using GIS. The overall vulnerability of Makassar City is calculated by considering the social, physical, economic, and environmental components, with different weighting factors to quantify their contributions to flood vulnerability. The weighting factors used in the vulnerability analysis are determined through the Analytic Hierarchy Process (AHP) process specific to the local context. The overall vulnerability index is shown in the equation as follows.

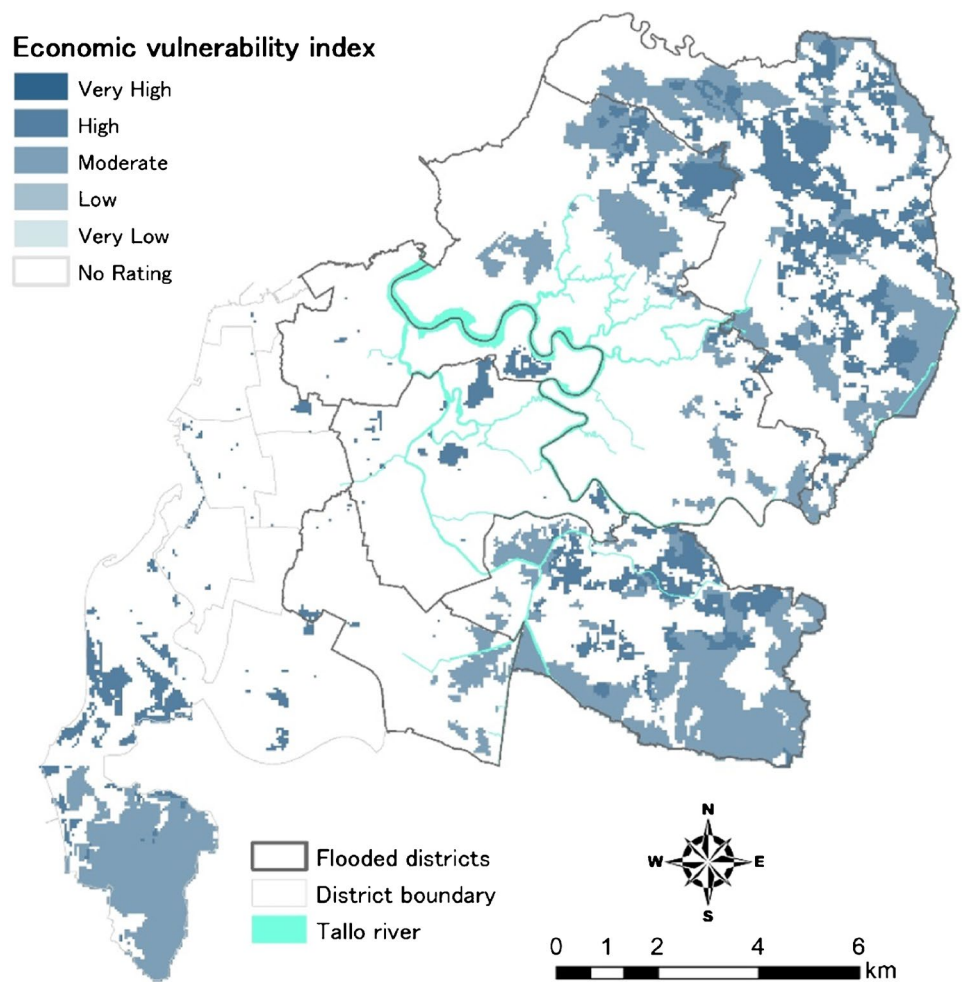
$$FVI = (VI_{\text{social}} \times 40\%) + (VI_{\text{physical}} \times 25\%) + (VI_{\text{economic}} \times 25\%) + (VI_{\text{environmental}} \times 10\%) \tag{6}$$

**Results**

**Social risk evaluation**

Statistics from 2012 were primarily utilized for population, population density, poverty ratio, age ratio, gender ratio, and disability ratio data (BPS 2012). These statistical data were input into the urban distribution areas at each sub-district. Figure 8 illustrates the flowchart of the GIS analysis used to calculate each indicator and obtain the social vulnerability score. Figure 9 shows the scoring results of individual indicators based on the data

**Fig. 16** Economic vulnerability score



input analysis on the map. The urban population density indicates high population densities ranging from 10,505 to 65,939 inhabitants/km<sup>2</sup>, with most of the city receiving high scoring values. The density map of Makassar City demonstrates that most sub-districts are densely populated. Among the scoring analysis results, ages, poverty, and people with disabilities (representing the group with the least capacity to recover from flood damages) show low vulnerability scores. Conversely, a high value of gender percentages is represented throughout the city. The combination of these five individual indicators gives the social vulnerability score (Fig. 10), with most sub-districts displaying social vulnerability to flooding varying from high to very high scores. Table 6 represents the risk calculation results obtained by multiplying the flood hazard scores and the social vulnerability scores for each sub-district. The specific risk index levels (very low (VL), low (L), moderate (M), high (H), and very high (VH)), along with the percentage area at those risk levels, are calculated in GIS. It can be identified that

some sub-districts, such as Antang, Sudiang Raya, Sudiang, and Tello Baru, stand out as being the most at risk in social aspects. Notably, the urban poor living along the coast and rivers are among the most vulnerable, as they reside in areas highly affected by current high flood depth. Flooding threatens their livelihoods and physical safety, further compounding the existing social vulnerabilities of low-income individuals.

**Physical risk evaluation**

The building features were drawn using spatial databases of the topology map and satellite images in 2012. This allowed for the analysis of the number of building points, areas, and types. The cost value of each building unit was justified based on the building types and area (rupiah per square meter). Local values were estimated using the building cost classification provided by the Ministry of Public Work (PU) of Indonesia (PU 2006). Figure 11 depicts the flowchart used to calculate

**Table 8** Risk assessment index for the economic component at the sub-district level

Sub-district	Area (ha)	Flood risk		Percentage area at risk levels (%)				
		Area (ha)	%	VL	L	M	H	VH
Bangkala	375.75	231	61	49	30	21		
Tamangapa	763.5	605.75	79	23	20	57		
Manggala	350.25	169.75	48	29	59	12		
Antang	531.25	158	30	59	19	11	11	
Batua	190	92.5	49	32	19	49		
Tamalanrea Indah	503.25	142	28	100				
Tamalanrea Jaya	375.5	273.25	73	88		12		
Tamalanrea	389.25	100.75	26	59	29	12		
Kapasa	669.25	51.25	8	54	28	18		
Parangloe	1080.25	7.5	1	100				
Bira	871.5	180	21	69	31			
Gunung Sari	375.25	81.25	22	81	19			
Karunrung	131.5	68	52	72	28			
Kassi Kassi	106.25	56.75	53	61	39			
Pampang	334.25	167	50	81		19		
Panaikang	304.25	160.25	53	100				
Paropo	127	27	21	100				
Tello Baru	162	48.25	30	78	3	19		
Buloa	95.25	4.5	5	100				
Tallo	62.75	6.25	10	100				
Lakkang	342.5	200.75	59	100				
Paccerrakkang	750	196	26	33	66	1		
Sudiang Raya	647.5	118.25	18	29		71		
Sudiang	623.75	33.25	5	54	2	44		

the physical vulnerability score. Three building factors were considered to determine the physical vulnerability values: houses, public facilities, and critical facilities. Figure 12 illustrates the scoring of individual indicators to estimate building cost values. Figure 13 shows the physical vulnerability score, indicating more than half of the city has susceptibility ranging from high to very high value. The central part of the city shows a high representation of physical vulnerability, while the northeast part exhibits lower scores. Table 7 provides the evaluation results of the physical risk in each sub-district. Sub-districts such as Sudiang, Tello Baru, and Antang are identified as having a high-risk level of flood-impacted areas in the physical aspect.

### Economic risk evaluation

To analyze the individual indicators for the economic component, a land cover map for 2012 was developed using a digital topographical map of 1:50.000 scales and satellite images. The land use division for agriculture was determined based on the detected land use boundaries from spatial data analysis. This division includes agriculture productive areas, such as paddy

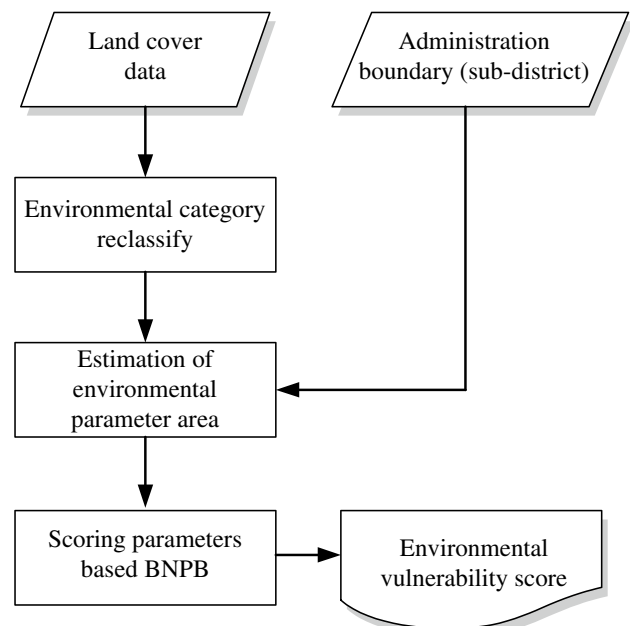


**Fig. 17** Flowchart of GIS analysis for calculating the environmental vulnerability score



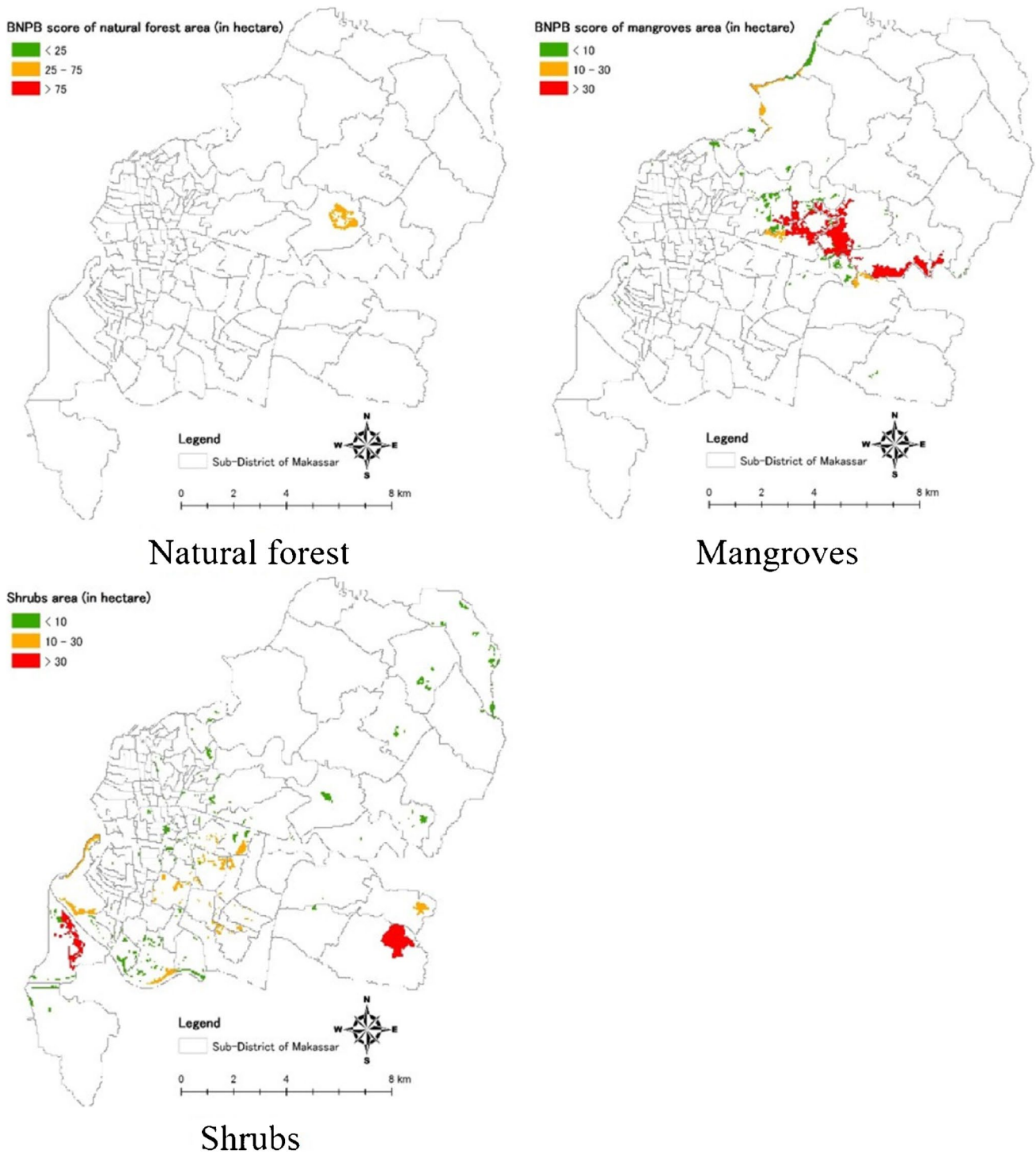
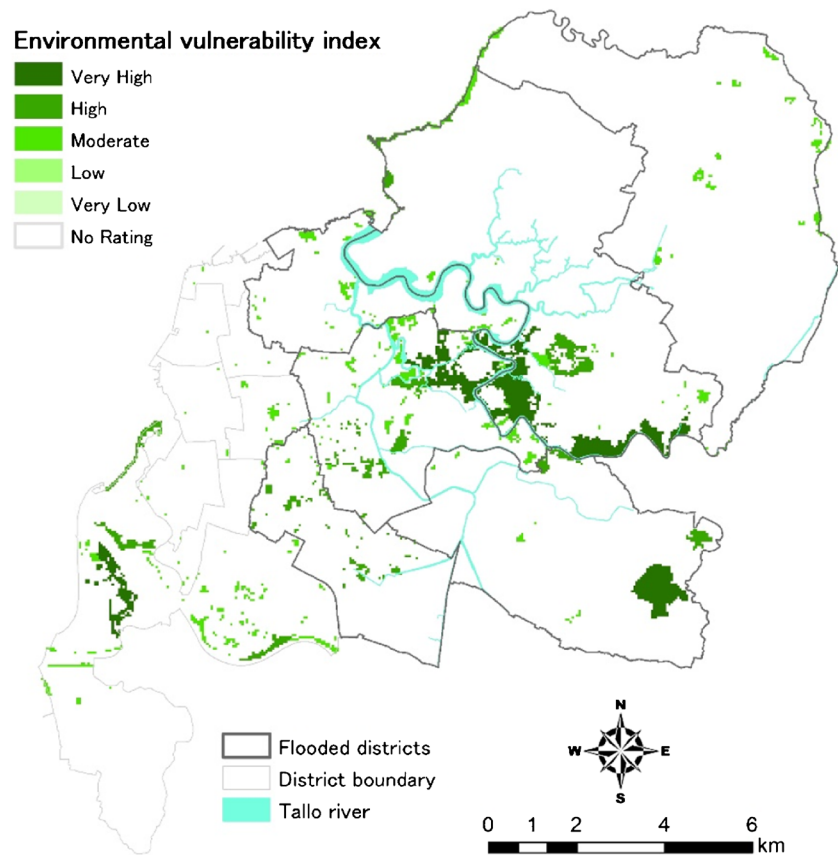


**Fig. 18** Scoring of individual indicator maps for the environmental vulnerability component

fields, garden fields, and mangrove fields. The productive land values and the land resource base (PDRB) values for each sub-district were obtained from the statistical database of Makassar City in 2012 and 2013.

Figure 14 illustrates the flowchart used to estimate the score of individual indicators related to economic vulnerability score, which is determined using two indicators (Fig. 15). Figure 16 shows that the economic

**Fig. 19** Environmental vulnerability score



aspect of Makassar City is fairly vulnerable to floods. Table 8 depicts that the highest percentage area at the high-risk level is located in the sub-district of Antang. Additionally, some sub-districts, such as Sudiang Raya, Tamangapa, Batua, Tamangapa, and Sudiang, exhibit a moderate vulnerability level, with most of the locations identified as productive lands, including paddy fields, garden fields, and fishponds. Notably, the paddy fields account for 36.34% of the total flood area and were significantly impacted. The expansion of urban areas from 1997 to 2012 has also contributed to the flood impacts on fishponds, affecting approximately 11.64% of the total flood area in 2013.

### Environmental risk evaluation

The environmental vulnerability assessment encompasses an analysis of natural forests, mangroves, and shrubs, which play a crucial role in mitigating ecological impacts in Makassar City. Figure 17 illustrates the flowchart of the environmental vulnerability score analysis. Relevant individual indicators are developed using the land cover data (Fig. 18), with vegetation covers predominantly found in

the vicinity of Tallo downstream, situated in the central part of Makassar City. Figure 19 presents the result of the environmental vulnerability score. Among the assessed components, mangroves are identified as the most at risk due to their high environmental exposure, limited storage capacity, and greater susceptibility to flooding. Both shrub and mangrove areas exhibit higher environmental vulnerability, covering approximately 84 to 138 hectares, respectively. Table 9 shows the distribution of the highest risks in the sub-districts of Panaikang, Tamalanrea Jaya, Pampang, and Tamangapa.

### Overall risk evaluation and verification

The overall risk index is determined by analyzing both the flood hazard score and the composite vulnerability score. The analysis reveals that Makassar City faces a moderate vulnerability level to floods, with over 50% of the areas categorized as having a low-risk flood index. Figure 20 shows the components of the flood risk index map and Fig. 21 shows the overall flood risk index map of Makassar City and the recorded casualty locations. Further details on the percentage of areas at different

**Table 9** Risk assessment index for the environmental component at the sub-district level

Sub-district	Area (ha)	Flood risk		Percentage area at risk levels (%)				
		Area (ha)	%	VL	L	M	H	VH
Bangkala	375.75	231	61	100				
Tamangapa	763.5	605.75	79	86				14
Manggala	350.25	169.75	48	92		8		
Antang	531.25	158	30	91			9	
Batua	190	92.5	49	100				
Tamalanrea Indah	503.25	142	28	48	1		51	
Tamalanrea Jaya	375.5	273.25	73	71			3	26
Tamalanrea	389.25	100.75	26	87	5		8	
Kapasa	669.25	51.25	8	100				
Parangloe	1080.25	7.5	1	100				
Bira	871.5	180	21	100				
Gunung Sari	375.25	81.25	22	100				
Karunrung	131.5	68	52	100				
Kassi Kassi	106.25	56.75	53	97	1	2		
Pampang	334.25	167	50	73		12		15
Panaikang	304.25	160.25	53	61	1	4		34
Paropo	127	27	21	100				
Tello Baru	162	48.25	30	83	17			
Buloa	95.25	4.5	5	94	6			
Tallo	62.75	6.25	10	92	8			
Lakkang	342.5	200.75	59	99	1			
Paccerrakkang	750	196	26	99	1			
Sudiang Raya	647.5	118.25	18	99		1		
Sudiang	623.75	33.25	5	100				

risk levels for each sub-district can be found in Table 10. Among the impacted areas, the sub-district of Antang is identified as having the highest risk level, mainly due to its degree of exposure to both social and physical aspects. Some sub-districts, such as Sudiang and Sudiang Raya, exhibit moderate risk levels, primarily attributed to their social and economic vulnerability to floods. Similarly, the sub-districts of Panaikang, Tamalanrea Jaya, Tamalanrea, and Tamangapa also have moderate risk levels, primarily influenced by environmental aspects. Overall risk evaluation results indicate that physical and environmental risk components significantly impact large areas at high-risk levels. Conversely, the lowest risks are sparsely distributed throughout the northeast and southeast sub-districts. Notably, the sub-districts of Lakkang and Bira in the vicinity of the Tallo downstream river display the lowest risk levels.

Due to the limited availability of detailed flood disaster damage information in Makassar City, the validation of the flood risk index obtained in this study was based on the affected location map of the January 2013 flood

disaster. This map illustrates the number of casualties or severely injured individuals during the disaster. It is expected that the affected locations accurately reflect the high-risk areas for flood disasters, particularly in the sub-districts of Antang, Kassi-kassi, Panaikang, Karunrung, and Tamalanrea Jaya. Figure 21 presents the overall flood disaster risk map overlaid with the vector layer of casualties from January 2013, and the casualties in each sub-district of different risk levels are summarized in Table 11. According to the data recorded by BPBD, the numbers of impacted individuals in the sub-districts of Kassi-Kassi, Panaikang Karunrung, and Tamalanrea Jaya were 10,961, 9651, 9532, and 8735 inhabitants, respectively. In total, 14 affected locations in Makassar City experienced moderate and high-risk levels, accounting for 71.4% of the total locations with casualties. The preliminary result indicates that the overall risk calculation of flood disasters at the sub-district level aligns well with the actual distribution of risk, demonstrating its high practical value.

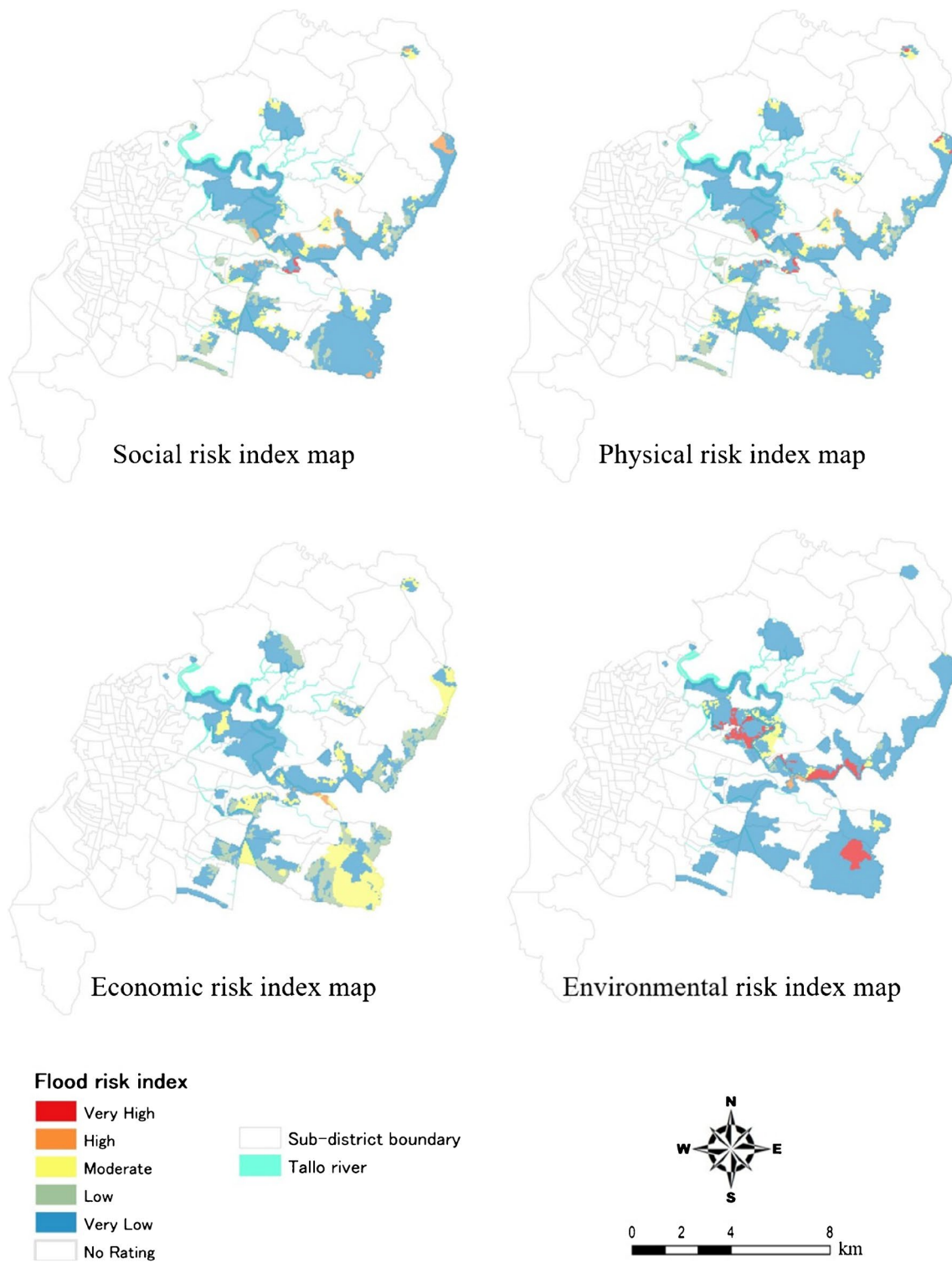


Fig. 20 Components of the flood risk index map

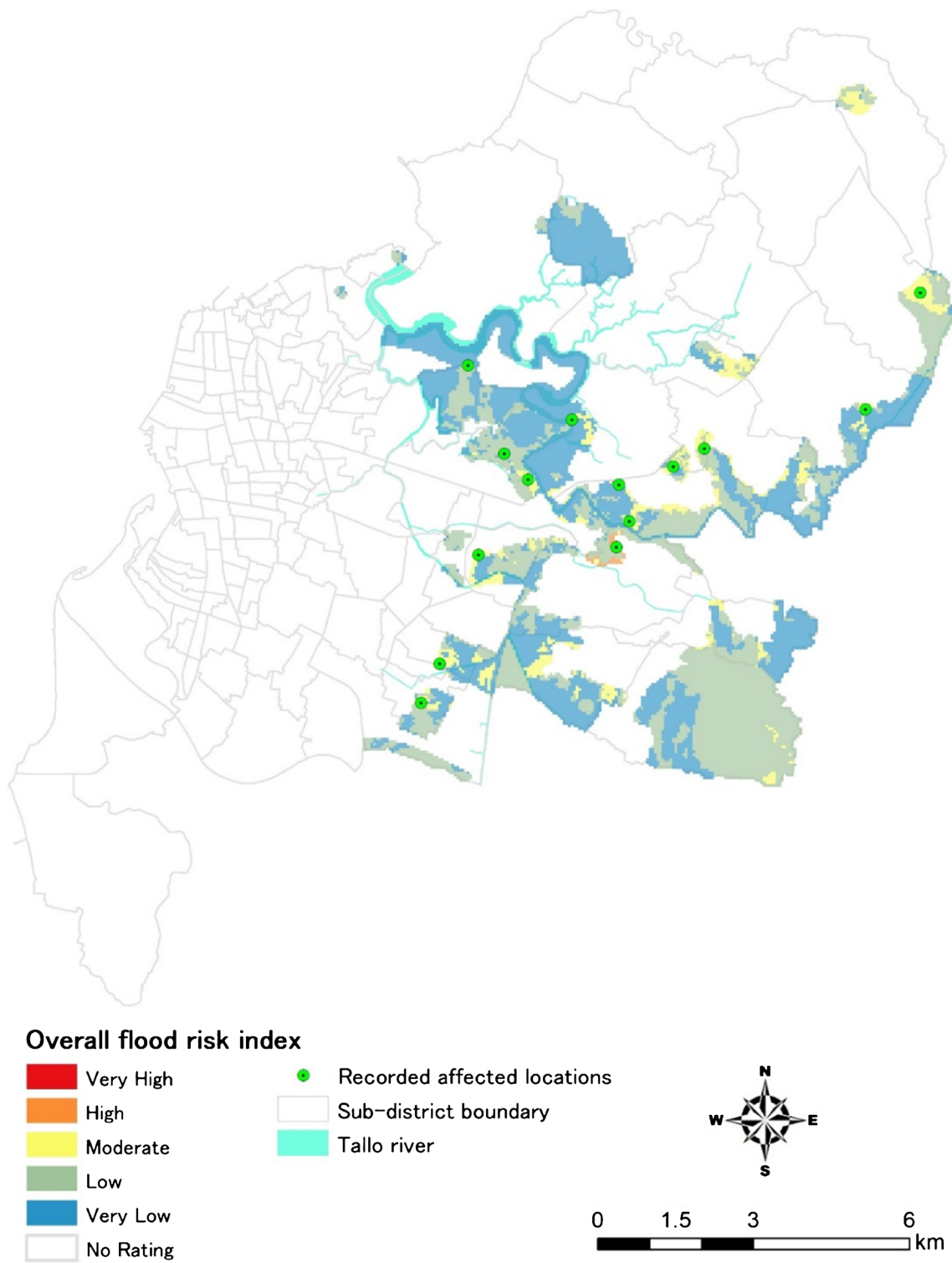


Fig. 21 Overall flood risk index map and recorded affected locations

**Table 10** Overall risk assessment index at the sub-district level

Sub-district	Area (ha)	Flood risk		Percentage area at risk levels (%)				
		Area (ha)	%	VL	L	M	H	VH
Bangkala	375.75	231	61	58	28	14		
Tamangapa	763.5	605.75	79	20	78	2		
Manggala	350.25	169.75	48	67	27	6		
Antang	531.25	158	30	34	58	1	7	
Batua	190	92.5	49	27	49	24		
Tamalanrea Indah	503.25	142	28	40	52	8		
Tamalanrea Jaya	375.5	273.25	73	37	47	16		
Tamalanrea	389.25	100.75	26	42	37	21		
Kapasa	669.25	51.25	8	28	28	44		
Parangloe	1080.25	7.5	1	27	73			
Bira	871.5	180	21	92	8			
Gunung Sari	375.25	81.25	22	40	49	11		
Karunrung	131.5	68	52	41	45	14		
Kassi Kassi	106.25	56.75	53	51	24	25		
Pampang	334.25	167	50	67	33			
Panaikang	304.25	160.25	53	45	51	4		
Paropo	127	27	21	14	86			
Tello Baru	162	48.25	30	47	34	19		
Buloa	95.25	4.5	5	39	61			
Tallo	62.75	6.25	10	32	68			
Lakkang	342.5	200.75	59	100				
Paccerrakkang	750	196	26	75	21	4		
Sudiang Raya	647.5	118.25	18	5	71	24		
Sudiang	623.75	33.25	5	6	43	51		

## Discussion

The main problems faced by developing countries are the limitation of disaster mitigation budgets, early warning systems, and information availability. This methodology aims to provide an accurate flood risk zonation that aligns with the actual disaster events. The study's results demonstrate a strong correlation with the onsite disaster survey conducted after the January 2013 flood in Makassar City. During the field survey, it was identified that the affected regions encompass the districts of Biringkanaya, Tamalanrea, Tallo, Manggala, Rappocini, and Panakukang, totaling more than 3000 hectares of flooded area. According to BPBD, the total number of affected individuals in these floods reached 101,972 inhabitants, with a significant concentration in the sub-districts of Kassi-Kassi, Panaikang, Karunrung, and Tamalanrea Jaya. Our analysis revealed that these same areas present the highest risk levels and thus should be given priority in hazard mitigation planning. By prioritizing areas based on the severity of the hazard, the methodology assists

the local government in devising appropriate plans and implementing accurate measurements for efficient mitigation efforts. This approach can also help in reducing the costs associated with rescue actions.

The calculation of the flood risk index serves the purpose of spatial planning and evaluating risk for disaster reduction in Makassar City. While the secondary datasets used as inputs at the sub-district level provide valuable information, they may not always be as accurate as locally surveyed data. To achieve a more precise risk value at the sub-district level, primary data for each vulnerability component should be considered for substitution where applicable. In this case study, the secondary datasets only cover the years 2012 and 2013. It is essential to note that the risk values represent an extrapolation based on this specific period. If data collection extends beyond this timeframe, variations in values may occur due to changes in local economic value and/or population density. The flood hazard map relies on an expected maximum flood area model derived from measurements taken in 2013. However, the available data for some risk

**Table 11** Verification of flood disaster risk assessment

Affected locations		Overall risk
District	Sub-district	
Biringkanaya	Paccerakkang	Moderate
	Sudiang Raya	Moderate
Manggala	Antang	High
	Batua	very low
Panakkukang	Panaikang	Moderate
	Panaikang	Moderate
	Pampang	Very low
Rappocini	Kassi-kassi	Moderate
	Karunrung	Moderate
Tamalanrea	Tamalanrea Jaya	Moderate
	Tamalanrea Jaya	Moderate
	Tamalanrea Jaya	Moderate
	Tamalanrea Indah	Very low
	Tamalanrea	Low

factors is rudimentary. To conduct a more comprehensive vulnerability analysis, the local methodological framework requires temporally and spatially granular statistical primary data. The processing of spatial statistical data is based on a grid-mesh system (50 m × 50 m), and localized inaccuracies in the source statistical data have the potential to propagate. As a result, the risk index map and its components should be considered as baseline measurements for determining flood risk at the sub-district level.

Furthermore, global climate change is expected to have an increasingly significant impact on coastal communities worldwide, including Makassar City. Some of these communities are already considered vulnerable to ongoing climatic variability (IPCC 2007). The projected effects of climate change include accelerated sea level rise, elevated tidal inundation, increased flood frequency, accelerated erosion, rising water tables, increased saltwater intrusion, more frequent storm surges, and increased cyclone occurrences (Fenster and Dolan 1996). Makassar City, including its coastline, is particularly susceptible to flooding, and this vulnerability may be exacerbated by changes in the occurrence of severe rainfall events in the future. Local conditions, such as low-lying lands and slow surface water drainage, further increase the risk of flooding. Currently, only approximately 50% of the surface water runoff area in Makassar City can be managed by the urban drainage systems. This highlights the need to enhance flood control measures, especially for urban constructions in high-risk areas, to mitigate

potential flood disaster losses. The flood risk index map provides a clear indication of safe and non-safe areas (50 m × 50 m) for urban development. As a result, it offers valuable information for land use planning and helps target areas that require prioritized risk reduction measures (Abuzied et al. 2016).

## Conclusions

In the GIS platform, the local methodological framework evaluates the social, physical, economic, and environmental aspects of the impacted areas. It identifies the flood risk levels across sub-districts in Makassar City. The methodology employs spatial and temporal analysis to generate a flood risk index map for the impacted area. It also analyzes the distribution of risk levels and severity percentages in the urban flood scenario of 2013. Spatial individual indicators, based on statistical and spatial data from the same period and relevant to vulnerability assessment in Makassar City, are generated. The flood risk index map is produced using recorded flood depth and area occurrence in 2013, along with historical flood hazard records. The study combines local indicators into a composite index, allowing geographical vulnerability and risk evaluation at a 50-m grid size, using a GIS grid-mesh system as the spatial treatment unit analysis. With the help of the flood risk index map, we determined that large flood-affected regions are classified at a low-risk index level, with risk components varying in intensity depending on the location. Despite limited information and resources for flood risk reduction, this study has enabled a better understanding of the affected regions. The suggested technique has produced a detailed and accurate flood risk map for Makassar City, which can be utilized for spatial urban planning and flood risk reduction. The map aids the local government in prioritizing risky zones that require greater attention.

**Author contribution** All authors contributed to the study's conception and design. Material preparation and data collection were performed by Poppy Indrayani and Ibrahim Djmaluddin. Interpretation of spatial data and analysis were performed by Poppy Indrayani, Ibrahim Djmaluddin, and Yue Cai. The first draft of the manuscript was written by Poppy Indrayani, and all authors commented on previous versions of the manuscript. All authors read and approved the final manuscript.

**Data availability** All data generated or analyzed during this study are included in this published article.

## Declarations

**Conflict of interest** The authors declare that they have no competing interests.

## References

- Abuzied S, Yuan M, Ibrahim S, Kaiser M, Saleem T (2016) Geospatial risk assessment of flash floods in Nuweiba area. *Egypt J Arid Environ* 133:54–72. <https://doi.org/10.1016/j.jaridenv.2016.06.004>
- Adger WN, Kelly PM (1999) Social vulnerability to climate change and the architecture of entitlements. *Mitig Adapt Strat G1* 43(4):253–266. <https://doi.org/10.1023/A:1009601904210>
- Ahmad SS, Simonovic SP (2013) Spatial and temporal analysis of urban flood risk assessment. *Urban Water J* 10(1):26–49
- Bigi V, Comino E, Fontana M, Pezzoli A, Rosso M (2021) Flood vulnerability analysis in urban context: a socioeconomic sub-indicators overview. *Clim* 9:12. <https://doi.org/10.3390/CLI9010012>
- National Agency for Disaster Countermeasure (BNPB) (2016) General guidelines of disaster risk assessment in Indonesia. Report. <https://bnpb.go.id/>
- Bose S, Mazumdar A (2023) Urban flood risk assessment and mitigation with InVEST-UFRM model: a case study on Kolkata city, West Bengal state (India). *Arab J Geosci* 16:320. <https://doi.org/10.1007/s12517-023-11412-2>
- Regional Disaster Management Agency (BPBD) (2014) Makassar City flood contingency plan, Makassar. Project Report. <https://bpbd.sulselprov.go.id/>
- The Central Bureau of Statistics of Makassar (BPS) (2012) Makassar data collection in 2012. Statistics of Makassar. Annual Report. <https://makassarkota.bps.go.id/>
- Chang H, Pallathadka A, Sauer J, Grimm NB (2021) Assessment of urban flood vulnerability using the social-ecological-technological systems framework in six US cities. *Sustain Cities Soc*: 68. <https://doi.org/10.1016/J.SCS.2021.102786>
- Chen W, Cutter SL, Emrich CT, Shi P (2013) Measuring social vulnerability to natural hazards in the Yangtze River Delta region. *China Int J Disast Risk Sc* 44(4):169–181. <https://doi.org/10.1007/S13753-013-0018-6>
- Chen W, Li Y, Xue W, Shahabi H, Li S, Hong H, Wang X, Bian H, Zhang S, Pradhan B, Ahmad BB (2020) Modeling flood susceptibility using data-driven approaches of naïve Bayes tree, alternating decision tree, and random forest methods. *Sci Total Environ* 701:134979. <https://doi.org/10.1016/j.scitotenv.2019.1349797>
- Cutter SL (1996) Vulnerability to environmental hazards. *Prog Hum Geog* 20:529–539. <https://doi.org/10.1177/030913259602000407>
- Cutter SL, Finch C (2008) Temporal and spatial changes in social vulnerability to natural hazards. *P Natl Acad Sci USA* 105:2301–2306
- Cutter SL, Boruff BJ, Shirley WL (2003) Social vulnerability to environmental hazards. *Soc Sci Quart* 84:242–261. <https://doi.org/10.1111/1540-6237.8402002>
- Dano UL, Balogun AL, Matori AN, Yusouf KW, Abubakar IR, Mohamed MAS, Aina YA, Pradhan B (2019) Flood susceptibility mapping using GIS-based analytic network process: a case study of Perlis. *Malaysia Water* 11(3):615. <https://doi.org/10.3390/w11030615>
- Darabi H, Choubin B, Rahmati O, Torabi HA, Pradhan B, Kløve B (2019) Urban flood risk mapping using the GARP and QUEST models: a comparative study of machine learning techniques. *J Hydrol* 569:142–154. <https://doi.org/10.1016/j.jhydrol.2018.12.002>
- Dintwa KF, Letamo G, Navaneetham K (2019) Measuring social vulnerability to natural hazards at the district level in Botswana. *J Disast Risk Stud* 11:1–11. <https://doi.org/10.4102/JAMBA.V11I11.447>
- Ehrlich PR, Holdren JP (1971) Impact of population growth. *Science* 171:212–217
- Fenster MS, Dolan R (1996) Assessing the impact of tidal inlets on adjacent barrier island shorelines. *J Coastal Res* 12:294–310
- Flanagan BE, Gregory EW, Hallisey EJ, Heitgerd JL, Lewis B (2011) A social vulnerability index for disaster management. *J Homel Secur Emerg*:8. <https://doi.org/10.2202/1547-7355.1792>
- Ghosh A, Kar SK (2018) Application of analytical hierarchy process (AHP) for flood risk assessment: a case study in Malda district of West Bengal, India. *Nat Hazards* 94:349–368. <https://doi.org/10.1007/s11069-018-3392-y>
- Hoyer J, Dickhaut W, Kronawitter L, Weber BH, Dickhaut J (2011) Water sensitive urban design: principles and inspiration for sustainable stormwater management in the city of the future. *Sustainable Water Management in the city of the Future, Integrated Project Report*
- Hu S, Cheng X, Zhou D (2017) GIS-based flood risk assessment in suburban areas: a case study of the Fangshan District, Beijing. *Nat Hazards* 87:1525–1543. <https://doi.org/10.1007/s11069-017-2828-0>
- Hufschmidt G (2011) A comparative analysis of several vulnerability concepts. *Nat Hazards* 58(2):621–643. <https://doi.org/10.1007/s11069-011-9823-7>
- Intergovernmental Panel on Climate Change (IPCC) (2007) IPCC Fourth Assessment Report. <http://www.ipcc.ch/ipccreports/ar4-wg1.htm>
- Iqbal A, Mondal SM, Veerbeek W, Shah AKM., Hakvoort H (2023) Effectiveness of UAV-based DTM and satellite-based DEMs for local-level flood modeling in Jamuna floodplain. *J Flood Risk Manag*:1–19. <https://doi.org/10.1111/jfr3.12937>
- Kasuni EA, Sangam S, Dhanika TR, Aakanchya B, Mohanasundaram S, Matthew ND (2021) Evaluation of artificial intelligence models for flood and drought forecasting in arid and tropical regions. *Environ Modell Softw* 144:105136. <https://doi.org/10.1016/j.envsoft.2021.105136>
- Khosravi K, Shahabi H, Pham BT, Adamowski J, Shirzadi A, Pradhan B, Dou J, Ly HB, Gróf G, Ho HL, Hong H, Chapi K, Prakash I (2019) A comparative assessment of flood susceptibility modeling using multi-criteria decision-making analysis and machine learning methods. *J Hydrol* 573:311–323
- Kim J, Gim THT (2020) Assessment of social vulnerability to floods on Java, Indonesia. *Nat Hazards* 102:101–114. <https://doi.org/10.1007/s11069-020-03912-1>
- Longley PA, Goodchild MF, Maguire DJ, Rhind DW (2001) *Geographic information systems and science*, 1st edn. John Wiley & Sons, Chichester, New York
- Meydelin IT, Dyah RH (2020) Urban resilience to floods in parts of Makassar, Indonesia. *The 1st Geosciences and Environmental Sciences Symposium (ICST 2020)*:200. <https://doi.org/10.1051/e3sconf/202020001007>
- Monirul M, Ajaya D, Ainun N (2003) Special issue on flood problems and management in South Asia: preface. *Nat Hazards* 28(1):7–9. <https://doi.org/10.1023/A:1021264130417>
- Muller A, Reiter J, Weiland U (2011) Assessment of urban vulnerability towards floods using an indicator-based approach—a case study for Santiago de Chile. *Nat Hazard Earth Sys* 11:2107–2123. <https://doi.org/10.5194/NHESS-11-2107-2011>
- Ngo PTT, Hoang ND, Pradhan B, Nguyen QK, Tran XT, Nguyen QM, Nguyen VN, Samui P, Bui DT (2018) A novel hybrid swarm optimized multilayer neural network for spatial prediction of flash floods in tropical areas using sentinel-1 SAR imagery and geospatial data. *Sensors* 18(11):3704. <https://doi.org/10.3390/s1811370432>
- Parasati H (2013) National Urban Development Program. Conference on e-Indonesia Initiative Forum IX/ 2013:1
- Public Work (PU) (2006) Regulation of the Minister of Public Works. Guidelines of technical requirements for buildings in Indonesia. Report. <https://www.pu.go.id/>
- Rana IA, Routray JK (2018) Multidimensional model for vulnerability assessment of urban flooding: an empirical study in Pakistan. *Int J Disast Risk Sc* 9:359–375. <https://doi.org/10.1007/s13753-018-0179-4>
- Rehman S, Sahana M, Hong H, Sajjad H, Ahmed BB (2019) A systematic review on approaches and methods used for flood vulnerability assessment: framework for future research. *Nat Hazards* 96:975–998. <https://doi.org/10.1007/s11069-018-03567-z>



- Riyanti D, Matthias G, Frank (2017) Disaster risk reduction in Indonesia: progress, challenges, and issues. Springer
- Roy S, Bose A, Chowdhury IR (2021) Flood risk assessment using geospatial data and multi-criteria decision approach: a study from historically active flood-prone region of Himalayan foothill. *India Arab J Geosci* 14:999. <https://doi.org/10.1007/s12517-021-07324-8>
- Rufat S, Tate E, Burton CG, Maroof AS (2015) Social vulnerability to floods: review of case studies and implications for measurement. *Int J Disast Risk Re* 14:470–486. <https://doi.org/10.1016/j.ijdr.2015.09.013>
- Sahraei R, Kanani-Sadat Y, Homayouni S, Safari A, Oubennaceur K, Chokmani K (2023) A novel hybrid GIS-based multi-criteria decision-making approach for flood susceptibility analysis in large ungauged watersheds. *J Flood Risk Manag* 16(2):1–26. <https://doi.org/10.1111/jfr.12879>
- Sandhyavetri A, Fatnanta F, Ramadhan, Husaini R, Suprayogi I (2019) Combination of a Coastal Vulnerability Index (CVI) and social economic approaches in prioritizing the development of Riau Coastlines, Indonesia. *MATEC Web Conf*:276. <https://doi.org/10.1051/mateconf/201927602006>
- Schmidtlein MC, Deutsch RC, Piegorsch WW, Cutter SL (2008) A sensitivity analysis of the Social Vulnerability Index. *Risk Anal* 28:1099–1114. <https://doi.org/10.1111/j.1539-6924.2008.01072.x>
- Siagian TH, Purhadi P, Suhartono S, Ritonga H (2014) Social vulnerability to natural hazards in Indonesia: driving factors and policy implications. *Nat Hazards* 70:1603–1617. <https://doi.org/10.1007/s11069-013-0888-3>
- Spielman S, Tuccillo J, Folch D, Schweikert A, Davies R, Wood NJ, Tate E (2020) Evaluating social vulnerability indicators: criteria and their application to the Social Vulnerability Index. *Nat Hazards* 100(1):417–436. <https://doi.org/10.1007/s11069-019-03820-z>
- Tate E, Rahman MA, Emrich CT, Sampson CC (2021) Flood exposure and social vulnerability in the United States. *Nat Hazards* 106:435–457. <https://doi.org/10.1007/s11069-020-04470-2/TABLES/6>
- Tehrany MS, Pradhan B, Jebur MN (2014) Flood susceptibility mapping using a novel ensemble weights-of-evidence and support vector machine models in GIS. *J Hydrol* 512:332–343. <https://doi.org/10.1016/j.jhydrol.2014.03.008>
- Tehrany MS, Lee MJ, Pradhan B, Jebur MN, Lee S (2014) Flood susceptibility mapping using integrated bivariate and multivariate statistical models. *Environ Earth Sci* 72(10):4001–4015. <https://doi.org/10.1007/s12665-014-3289-3>
- Tehrany MS, Pradhan B, Jebur MN (2015a) Flood susceptibility analysis and its verification using a novel ensemble support vector machine and frequency ratio method. *Stoch Env Res Risk A* 29(4):1149–1165. <https://doi.org/10.1007/s00477-015-1021-9>
- Tehrany MS, Pradhan B, Mansor S, Ahmad N (2015) Flood susceptibility assessment using GIS-based support vector machine model with different kernel types. *CATENA* 125:91–101. <https://doi.org/10.1016/j.catena.2014.10.017>
- Ullah K, Zhang J (2020) GIS-based flood hazard mapping using relative frequency ratio method: a case study of Panjkora River Basin, eastern Hindu Kush, Pakistan. *Plos One* 15(3):e0229153. <https://doi.org/10.1371/journal.pone.0229153>
- United Nations Development Programme (UNDP) (2004) Reducing disaster risk: a challenge for development. Bureau for Crisis Prevention and Recovery (BRCP), New York, John S. Swift. [www.undp.org/bcpr](http://www.undp.org/bcpr)
- UN-Habitat (2014) Cities and climate change initiative: Makassar, Indonesia. *Climate Change Vulnerability Assessment*. [www.unep.org/roap](http://www.unep.org/roap)
- United Nations Office for Disaster Risk Reduction (UNISDR) (2017) Flood hazard and risk assessment. In: *Words into action guidelines: national disaster risk assessment hazard specific risk assessment*. Geneva
- Wang RQ (2021) Artificial intelligence for flood observation. *Earth Observation for Flood Applications*:295–304. <https://doi.org/10.1016/B978-0-12-819412-6.00013-4>
- White L (2008) The absorbent city: urban form and flood risk management. *Urban Des Plann* 161(4):151–161
- Zalnezhad A, Rahman A, Nasiri N, Haddad K, Rahman MM, Vafakhah M, Samali B, Ahamed F (2022) Artificial intelligence-based regional flood frequency analysis methods: a scoping review. *Water* 14(17):2677. <https://doi.org/10.3390/w14172677>

Springer Nature or its licensor (e.g. a society or other partner) holds exclusive rights to this article under a publishing agreement with the author(s) or other rightsholder(s); author self-archiving of the accepted manuscript version of this article is solely governed by the terms of such publishing agreement and applicable law.